Joint Pathology Center

Veterinary Pathology Services

WEDNESDAY SLIDE CONFERENCE 2016-2017

C o n f e r e n c e 22

5 April 2017

CASE I: 2671-16 (JPC 4081675).

Signalment: 10-days-preterm, male, cynomolgus macaque fetus (*Macaca fascicularis*).

History: A male cynomolgus macaque fetus was aborted from an 8-year-old female multiparous dam macaque of Vietnam origin. The female macaque had not undergone any experimental procedures or manipulations and was used as a control animal for pregnancy and infant developmental study. The dam was in good general health and was negative for Herpes B, SRV, SIV, STLV, tuberculosis, and parasites on routine health monitoring. The dam was mated to a breeding male cynomolgus macaque and pregnancy was confirmed by ultrasound diagnosis with the visualization of the gestational sac. At gestation day GD60, a large anechoic, abnormal round cystic space was observed in the abdominal region of the developing fetus. Abnormalities were not apparent on subsequent ultrasound scans at GD90 and GD120. The fetus had a viable heart beat up to the final ultrasound scan at GD120, before abortion occurred at GD146 (about ten days before estimated due date).

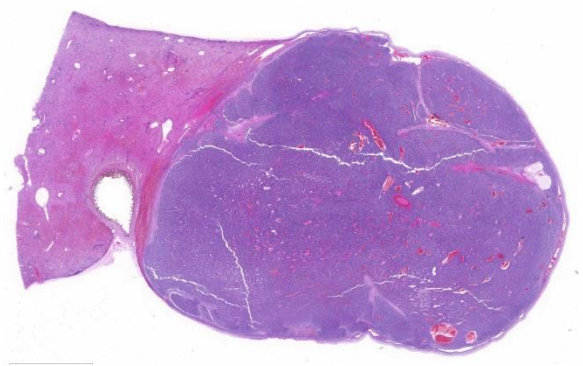

Liver, cynomolgus abortus: The liver is focally expanded by a nodular, moderately cellular neoplasm. (HE, 6X)

Gross Pathology: The fetus was presented dead with umbilical cord and placenta intact. On external examination, there was severe congestion of the head indicating dystocia at birth, likely caused by an enlarged fetal abdominal circumference resulting in difficult passage through pelvic canal. Meconium was present in the fetal fluid which indicated fetal stress at birth and confirmed that animal was alive during birth. Abdominal cavity contained a large amount of blood-tinged fluid. The fetus had

a large liver mass and a cystic structure attached to the left abdominal wall.
At necropsy and examination of visceral organs, expanding the right border of the right median liver lobe, compressing hepatic parenchyma and adjacent gallbladder was a 4cm x 1.7cm x 2.1cm, white to light brown nodular mass. Nodules of this neoplasm were surrounded by fibrovascular tissue, and the neoplasm was well-demarcated and encapsulated.

Laboratory results: None

Histopathologic Description: Histologically, neoplasm in the right median liver lobe was characterized by an expansile and fairly well-demarcated proliferation of neoplastic cells, arranged in sheets, cords and packets with primitive tubular and acinar formations, separated by fibrovascular stroma. Cells are polygonal, have well-defined cell borders, and often form pseudorosettes. Neoplastic cells are 10-15 µm in diameter, have high nuclear to cytoplasmic ratio, pale vesiculate eosinophilic to basophilic cytoplasm, central round to oval moderately stippled nuclei with 1-2 nucleoli. Large numbers of extramedullary hematopoietic cells are present between the cords and packets of neoplastic cells. The neoplastic cells have strong diffuse positive cytoplasmic immunolabelling for pancytokeratin (MNF116), cytokeratin 18 and alpha-fetoprotein, strong membrane and moderate to weak cytoplasmic beta-catenin immuno-labelling. The neoplastic cells are diffusely negative for vimentin, chromogranin-A, neuron specific enolase (NSE). Histopathology and immunohistochemistry results indicate a hepatoblastoma of embryonal subtype for this neoplasm.

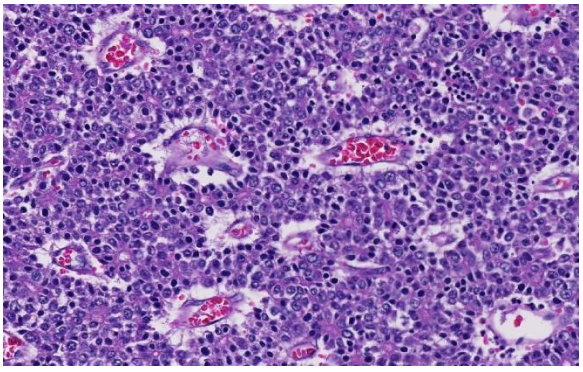

Liver, cynomolgus abortus: Neoplastic cells are polygonal to pyramidal and often palisade around blood vessels (pseudorosette formation.) (HE 240X)

Contributor's Morphologic Diagnosis: Macaque fetal liver: Hepatoblastoma (embryonal subtype).

Contributor's Comment: Hepatoblastoma (HBL) is a malignant tumor that arises from embryonic and fetal hepatocytes and is comprised of mixed epithelial, mesenchymal, undifferentiated components, and typically classified into two categories of epithelial or mixed epithelial-mesenchymal.[1,2] Epithelial HBL is subcategorized into fetal, mixed fetal-embryonal (most common), macrotrabecular and anaplastic small cell types, while the mixed type contains immature mesenchymal components. [5,6] These tumor subtypes, among other pediatric liver tumors, are well-illustrated in a fairly recent publication by Tanaka Y, 2013.[8] In humans, HBL is the most common pediatric liver malignancy and is usually diagnosed within the first three years of life. About two-thirds of liver masses are malignant in children and approximately 70% of these are hepatoblastomas or hepatocellular carcinomas.[2]

Hepatoblastoma is a rare tumor in domestic animals and have been reported in the dog, alpaca, horse, mouse, and cat. [6,8,9,10,11,12,13,14] While other induced and naturally occurring hepatic tumors have been reported in cynomolgus macaques, hepatoblastoma is a tumor that has not been reported in literature from this species.

Hepatoblastomas and their subtypes in humans can be further characterized by immunohistochemistry markers such as alpha fetoprotein (AFP), glypican 3 (GPC3), carbamoyl phosphate synthetase 1 (CSP1), vimentin, cytokeratin and beta-catenin. [2, 7] Classification of the hepatic tumor in this fetal macaque tumor was attempted based on the neoplastic cell morphology and immunohistochemistry results using the recently published classification for pediatric liver tumor by López-Terrada D.[2]

AFP is expressed in normal, non-neoplastic human fetal liver and is also seen in human liver tumors and some germ cell tumors. In this study, AFP was weakly expressed by hepatocytes of liver parenchyma adjacent to the hepatoblastoma, while strong positive AFP immunolabelling by neoplastic cells of the hepatoblastoma highlighted architecture of the neoplastic embryonal hepatocytes and supported diagnosis of embryonal subtype of hepatoblastoma for this fetus's liver tumor. As AFP is also a secreted protein, increased background and serum labeling of AFP could also be seen in immuno-histochemically labeled sections, [7] and was also noted in blood vessels of AFP labeled sections of this fetal macaque's tumor. While AFP is currently the most reliable and consistent marker in hepatoblastoma,[4] approximately 5-10% of human hepato-blastomas are negative for AFP and other markers such as Delta-like homolog (DLK1) are being investigated as potential serum markers for diagnosis of this tumor.[15]

Pancytokeratin expression in human hepatoblastomas can be variable while vimentin is negative on the epithelial components.[7] Cytokeratin 18 (CK18) is expressed in adult epithelial tissues such as liver, lung, kidney, pancreas, gastrointestinal tract, mammary glands and their associated tumors, and an increased CK18 expression in several cancer types of human patient is linked to poorer prognosis.[16] In this study, the strong positive pancytokeratin and CK18 expression by the fetal hepatic neoplasm are consistent with hepatocyte lineage of the neoplastic cells. The negative and much smaller tumor area of vimentin labeling on the mesenchymal components of the liver tumor, in this case, indicate a hepatoblastoma with predominant epithelial cell component.

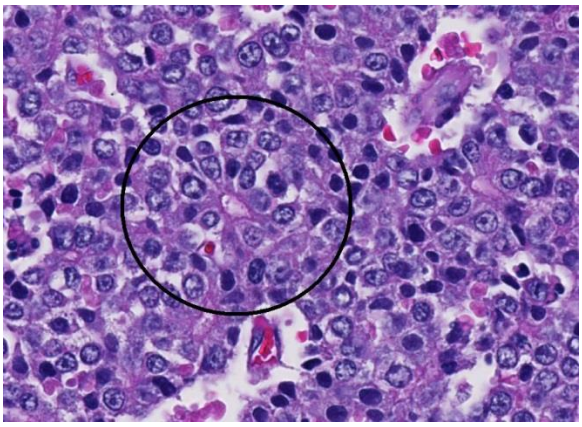

Liver, cynomolgus abortus: Neoplastic cells rarely form true rosettes (circled). (HE 400X)

Hepatoblastomas in both humans and mouse have high prevalence of deletion mutation in GSK-3β binding region of β-catenin gene of Wnt signalling pathway, with approximately 80-90% of hepatoblastomas in humans having mutations in beta-catenin (CTNNB1).[2, 7, 17] The nuclear and/or cytoplasmic pattern of expression of β-catenin could be used to distinguish between neoplastic hepatic and biliary hepatocytes. [2, 7] Specifically, non-neoplastic hepatocytes and biliary epithelium have only distinct membranous beta-catenin labeling, while cytoplasmic expression of beta-catenin indicates the epithelial cells of neoplastic nature.[2, 7]

Neoplastic cells of the liver, in this case, have cytoplasmic beta-catenin immunolabelling.
Based on histopathology findings and positive pancytokeratin (MNF116), cytokeratin 18, alpha-fetoprotein, as well as the cytoplasmic beta-catenin immunohistochemistry results, current findings are indicative of an embryonal subtype of hepatoblastoma in the liver of this macaque fetus.

JPC Diagnosis: Liver: Hepatoblastoma, cynomolgus macaque fetus, *Macaca fascicularis*.

Conference Comment: The contributor provides an outstanding review of the immunohistochemical staining characteristics of hepatoblastomas in a fetal cynomolgus macaque. Hepatoblastomas are thought to be derived from the pluripotential stem cell progenitor cells in the liver and usually occur in very young or fetal animals, as in this case; although there are rare reports in adults.[4,7] As in other embryonal neoplasms reported in animals, such as nephroblastomas, neuroblastomas, and medulloblastomas, hepatoblastomas are composed of primitive poorly differentiated blastic cells.[7,18] Participants noted the prominent arrangement of neoplastic cells into rosettes, pseudorosettes, sheets, and solid cords separated by variably sized vascular spaces.[3,4,7] Although not a prominent feature in this case, some reported hepatoblastomas can display squamous, chondrous, or osseus metaplasia, which reflect the ability the ability of this neoplasm to have widely divergent differentiation. In animals and humans, these neoplasms are classified in epithelial (fetal or embryonal), mesenchymal, and mixed patterns with combinations of neoplastic cell types occurring within a single neoplasm. The fetal form is composed of large polygonal cells with abundant vacuolated eosinophilic cytoplasm. The embryonal form is composed of smaller neoplastic polygonal cells arranged in ribbons and rosettes and is the predominant form featured in this case.[4] Human epithelial hepatoblastomas are further categorized into fetal, embryonal and mixed, macrotrabecular, or anaplastic small cell types.[4,7] The fetal macrotrabecular subtype can appear remarkably similar to hepatocellular carcinoma, with trabeculae of neoplastic cells piling up to ten layers thick. The Anaplastic small cell subtype is arranged in sheets and is difficult to distinguish from the other blastic neoplasms mentioned above. Mesenchymal subtypes are mainly comprised of undifferentiated spindle cells, cartilage, bone, or striated muscle.[4,7,18]

Conference participants noted that there is a marked increase in extramedullary hematopoiesis (EMH) as characterized by erythroid precursor cells and megakaryocytes within the solid portions of the mass when compared to the normal adjacent liver parenchyma. This is a commonly reported phenomenon of this neoplasm. Although EMH is not uncommon in the fetal liver, the marked increase within the neoplasm compared to the normal liver tissue stimulated some discussion among attendees. The molecular pathogenesis of EMH within hepatoblastomas is not yet known; however, it is thought that the primitive neoplastic cells may retain the CD34 positive multipotential nature of bone marrow origin cells and can differentiate into erythroid precursors and megakaryocytes under the influence of hematopoietic cytokines such as IL-6, G-CSF, and GM-CS.[15] The presence of EMH within the neoplasm can assist in differentiating hepatocellular carcinoma and macrotrabecular hepatoblastoma, which can have a similar morphology.[15]

Contributing Institution:
Advanced Molecular Pathology Laboratory
Institute of Molecular and Cell Biology
Proteos, Singapore

References:

1. Ano N, Ozaki K, Nomura K, Narama I. Hepatoblastoma in a cat. *Vet Pathol*. 2011; 48(5):1020-3.
2. De Vries C, Vanhaesebrouck E, Govaere J, Hoogewijs M, Bosseler L, Chiers K, Ducatelle R. Congenital ascites due to hepatoblastoma with extensive peritoneal implantation metastases in a premature equine fetus. *J Comp Pathol*. 2013 Feb;148(2-3):214-9.
3. Cullen JM. Tumors of the liver and gallbladder. In: Meuten DJ, ed. *Tumors in Domestic Animals*. 5th ed. Ames, IA: Wiley Blackwell; 2017:853-855.
4. Cullen JM, Stalker MJ. Liver and biliary system. In: Maxie MG, ed. *Jubb, Kennedy and Palmer's Pathology of Domestic Animals*. Vol 2. 6th ed. Philadelphia, PA: Elsevier Ltd; 2016:347-348.
5. Falix FA, Aronson DC, Lamers WH, Hiralall JK, Seppen J. DLK1, a serum marker for hepatoblastoma in young infants. *Pediatr Blood Cancer*. 2012 Oct;59(4):743-5.
6. Helmberger TK, Ros PR, Mergo PJ, Tomczak R, Reiser MF. Pediatric liver neoplasms: a radiologic-pathologic correlation. *Eur Radiol*. 1999;9(7):1339-47.
7. Kim Y, Sills RC, Houle CD. Overview of the molecular biology of hepatocellular neoplasms and hepatoblastomas of the mouse liver. *Toxicol Pathol*. 2005; 33(1):175-80.
8. López-Terrada D, Alaggio R, de Dávila MT, Czauderna P, Hiyama E, Katzenstein H, Leuschner I, Malogolowkin M, Meyers R, Ranganathan S, Tanaka Y, Tomlinson G, Fabrè M, Zimmermann A, Finegold MJ; Children's Oncology Group Liver Tumor Committee. Towards an international pediatric liver tumor consensus classification: proceedings of the Los Angeles COG liver tumors symposium. *Mod Pathol*. 2014 Mar;27(3):472-91.
9. Loynachan AT, Bolin DC, Hong CB, Poonacha KB. Three equine cases of mixed hepatoblastoma with teratoid features. *Vet Pathol*. 2007 Mar;44(2):211-4.
10. Neu SM. Hepatoblastoma in an equine fetus. *J Vet Diagn Invest*. 1993 Oct;5(4):634-7.
11. Nonoyama T, Fullerton F, Reznik G, Bucci TJ, Ward JM Nonoyama T, Fullerton F, Reznik G, Bucci TJ, Ward JM: Mouse hepatoblastomas: a histologic, ultrastructural, and immunohistochemical study. *Vet Pathol*. 25: 286–296, 1988
12. Nonoyama T, Reznik G, Bucci TJ, Fullerton F. Hepatoblastoma with squamous differentiation in a B6C3F1 mouse. *Vet Pathol*. 1986 Sep;23(5):619-22.
13. Shiga A, Shirota K, Shida T, Yamada T, Nomura Y. Hepatoblastoma in a dog. *J Vet Med Sci*. 1997 Dec;59(12):1167-70.
14. Tanaka Y, Inoue T, Horie H. International pediatric liver cancer pathological classification: current trend. *Int J Clin Oncol*. 2013 Dec;18(6):946-54.
15. Thambi R, Lekshmi D, et al. Extramedullary hematopoiesis as a clue to diagnosis of hepatoblastoma on fine needle aspiration cytology: A

report of two cases. *J Cytol*. 2013; 30(3):198-200.
16. Watt BC, Cooley AJ, Darien BJ. Congenital hepatoblastoma in a neonatal alpaca cria. *Can Vet J*. 2001 Nov;42(11):872-4.
17. Weng YR, Cui Y, Fang JY. Biological functions of cytokeratin 18 in cancer. *Mol Cancer Res*. 2012 Apr;10(4):485-93.
18. Wright JR Jr, Pinto-Rojas A, Trevenen CL, Yu W. Teratoid features in mixed hepatoblastoma. *Vet Pathol*. 2010 Sep;47(5):1003-4.

CASE II: MS1602402 (JPC 4087117).

Signalment: Four-month-old female arginase vasopressin receptor knock-out (V1aR KO) mouse (*Mus musculus*).

History: This breeder female mouse was found to have dystocia. It was treated with subcutaneous fluids and was subsequently euthanized.

Gross Pathology: A female 4-month-old black mouse was submitted following euthanasia. The subcutaneous tissues were mildly dry. The mouse was pregnant with two full term fetuses present within the left uterine horn and none present in the right uterine horn. The pubis was poorly dilated. The two fetuses within the left uterine horn appeared to be mild to moderately autolyzed, consistent with fetal death in utero. A placental disc was present associated with each fetus and five additional placental discs were present within the left uterine horn. The heart, lungs, liver, kidneys, spleen and GI tract appeared normal.

Laboratory results: A bacterial culture obtained from the uterus yielded *Pasteurella pneumotropica*, *Enterococcus faecalis* and *Enterococcus gallinarum*.

Histopathologic Description: Microscopic examination revealed a moderate acute suppurative placentitis with bacterial colonies of coccobacilli associated with the

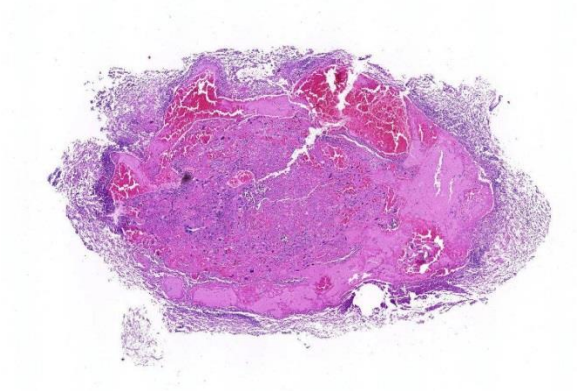

Placenta, mouse. Normal hemochorial placental architecture is effaced by large areas of hemorrhage and necrosis. The allantochorion is arrayed around the placenta as a result of placement in the cassette. (HE, 16X)

inflammation. Moderate numbers of degenerative neutrophils were present along the maternal and fetal margins of the placenta. Some sections had neutrophilic foci within the placenta. Mild multifocal mineralization was noted within the placental disc. Moderate diffuse mineralization of the placental labyrinth capillary walls was evident and confirmed by von Kossa stain. Some sections included placental membranes with a moderate necrosuppurative amniochorionitis evident, associated with coccobacilli. Coccobacilli are gram-negative on gram stains.

There was moderate to severe multifocal necrosuppurative endometritis with bacterial colonies present associated with the uterine inflammation. One of the two fetuses examined had moderate autolysis consistent with death in utero, with no evidence of inflammation or bacteria. No other significant lesions were noted.

Contributor's Morphologic Diagnosis: 1. Placenta, placentitis, acute, suppurative, moderate to severe, with gram-negative coccobacilli.
2. Placental labyrinth capillaries, mineralization, diffuse, moderate
3. Placental membranes, amniochorionitis, necrosuppurative, acute, moderate to severe

Contributor's Comment: Morbidity, in this case, was due to endometritis, placentitis, and fetal death in utero due to reproductive tract infection with *Pasteurella pneumotropica*. *Pasteurella pneumotropica* is a non-motile, gram-negative cocco-bacillus. Diagnosis is usually by bacterial culture or PCR analysis. It grows well on blood agar under aerobic conditions with 7-10% CO2 at 37 degrees Celsius.[12] It is non-hemolytic, oxidase, catalase, urease and indole positive and ferments glucose, sucrose, and maltose without gas production.[7] Two biotypes, Heyl and Jawetz, have been described and can be differentiated by PCR.[7,12]

Pasteurella pneumotropica is generally considered an opportunistic agent and some degree of immunodeficiency often plays a role in disease pathogenesis.[8] It has been isolated from the skin, conjunctiva, nasopharynx, trachea, lung, intestinal tract, vagina, uterus, urinary bladder, prepuce, preputial glands, bulbourethral glands and seminal vesicles in asymptomatic and clinically affected mice.[6,13] Infections have been reported in mice, rats, guinea pigs, hamsters, cotton rats, rabbits, dogs, cats and humans.[1] The agent can infect the vaginal tract and ascend to the uterus causing infertility associated with metritis, abortion and stillbirths.[1]

The primary route of infection is by direct contact with oropharyngeal or reproductive tract secretions.[12] Mice and rats with infected uteri are typically found in colonies known to have a positive incidence of *Pasteurella pneumotropica* in the upper respiratory tract.[3] Bacterial toxins PnxlA,llA and lllA have been identified on infected cell surfaces and are associated with adhesion to extracellular matrix and virulence. These toxins may also act as leukotoxins and disrupt actin cytoskeleton.[11]

Treatment in drinking water with enrofloxacin (Baytril) a broad spectrum, bactericidal, fluoroquinolone antibiotic has been used effectively to eliminate *Pasteurella pneumotropica* from infected mice.[12]

The finding of diffuse mineralization of placental labyrinth capillaries was interesting. This may be a manifestation of dystrophic calcification, and associated

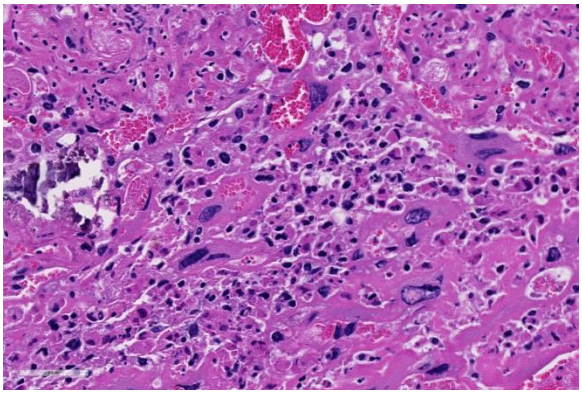

Placenta, mouse. Chorionic villi are separated by moderate amounts of degenerate neutrophils admixed with fibrin and cellular debris. There is crystalline mineral at left. (HE, 324X)

ineffective placental circulation may be a direct cause of fetal death in utero in this case.

JPC Diagnosis: Placenta and membranes: Placentitis and amniochorionitis, necrotizing, multifocal to coalescing, moderate, with colonies of coccobacilli, V1aR KO mouse, *Mus musculus*.

Conference Comment: Prior to discussing this case, the conference moderator led a

discussion on the normal placentation in mice. Both rats and mice have a hemochorial and discoid type of placenta.[2,4,9] In this type of placentation, maternal blood comes into direct contact with the fetal chorion, which does not occur in epitheliochorial placentation of ruminants and endotheliochorial placentation of dogs and cats.[2,4] Histologically, the mouse placenta is composed of the labyrinth and basal zones, the decidua, and the metrial glands. The labyrinth zone is composed of three layers of trophoblasts which separate maternal and fetal vasculature. The outer layer is composed of cyntrophoblasts, which directly contact maternal blood and has a microvillous surface. Beneath this layer are two layers of syncytiotrophoblasts.[4]

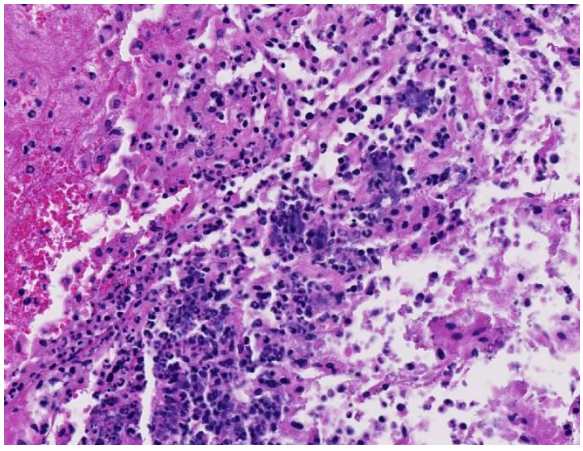

Placenta, mouse. Placental membranes are multifocally effaced by aggregates of degenerate neutrophils and colonies of bacilli. (HE, 324X)

Subjacent to the labyrinth zone is the basal zone which is composed of spongio-trophoblasts, trophoblastic giant cells, and glycogen cells. Spongiotrophoblasts are located at the maternal and fetal interface between the trophoblastic giant cell and inner labyrinth layer.[4] The trophoblastic giant cells are large pleomorphic cells that show extensive DNA replication and can have the equivalent of up to 1000 copies of the genome within a single cell.[4,6] These cells are vital for implantation and secretion of a wide array of hormones. Care should be taken to not interpret these cells as anaplastic tumor giant cells.[6] Glycogen cells have abundant intracytoplasmic glycogen and usually disappear prior to parturition. The origin and function of the glycogen cells is unknown. The decidua is composed of the maternal endometrial lining cells that are responsible for the exchange of nutrients, gas, and waste products between the fetus and the dam.[2,4,6] Finally, the metrial gland is present in the mesometrial triangle of the gravid mouse uterus and contains granulated endometrial gland cells (GMG), endometrial stromal cells, blood vessels, trophoblasts, and fibroblasts. Granulated mesometrial gland cells are bone marrow derived perforin-positive, natural killer cells that proliferate within the metrial gland upon pregnancy in mice. In health, GMG are mitotically active and often binucleated. The exact function of these cells has not yet been fully elucidated.[4,10]

Conference participants noted some moderate slide variation in this case, as some sections contain only the placental disk with no sections of the placental membrane or attached uterus. Additionally, the dystrophic mineralization of the capillaries within the placental labyrith, mentioned by the contributor, is not as prominent on every examined slide. Conference participants readily identified areas of lytic necrosis with moderate numbers of infiltrating neutrophils centered on small colonies of coccobacilli. *Pasteurella pneumotropica* is a common opportunistic pathogen in mice and infection often produces subclinical disease in immune competent mice.[9] The increased use of immunosuppressed strains of mice, however, has contributed to an increase in the incidence of clinical disease. Typically, it is implicated as a cause of severe pneumonia (hence its name), but has been

rarely reported as a cause of a wide variety of necrotizing and suppurative lesions, including those leading to infertility, reproductive failure and abortion, as in this case.[9] Most immunocompetent rats and mice with clinical respiratory disease are co-infected with Sendai virus, *Mycoplasma pulmonis*, cilia-associated respiratory (CAR) bacillus, *Streptococcus pneumoniae*, *Corynebacterium kutscheri*, *Bordetella bronchiseptica*, or *Klebsiella pneumonia*e as part of the chronic respiratory disease syndrome.[9]

Contributing Institution:
National Institutes of Health
Division of Veterinary Resources
Bethesda, Maryland, USA

References:

1. Ackerman JI, Fox JG. Isolation of *Pasteurella ureae* from reproductive tracts of congenic mice. *J Clin Microbiol*. 1981; 13(6):1049-53.
2. Bacha WJ, Bacha LM. *Color Atlas of Veterinary Histology*. 3rd ed. Baltimore, MD: Lippincott Williams & Wilkins; 2012:243-260.
3. Blackmore DK, Casillo S. Experimental investigation of uterine infections of mice due to *Pasteurella pneumotropica*. *J Comp Pathol*. 1972; 82(4):471-5.
4. Furukawa S, Kuroda Y, et al. A comparison of the histological structure of the placenta in experimental animals. *J Toxicol Pathol*. 2014; 27(1):11-18.
5. Hooper A, Sebesteny A. Variation in *Pasteurella pneumotropica*. *J Med Microbiol*. 1974; 7(1):137-40.
6. Hu D, Cross JC. Development and function of trophoblast giant cells in the rodent placenta. *Int J Dev Biol*. 2010; 54(3):341-354.
7. Kawamoto E, Sasaki H, Okiyama E, Kanai T, Ueshiba H, Ohnishi N, Sawada T, Hayashimoto N, Takakura A, Itoh T. Pathogenicity of *Pasteurella pneumotropica* in immunodeficient NOD/ShiJic-scid/Jcl and immunocompetent Crlj: CD1 (ICR) mice. *Exp Anim.* 2011;60(5):463-70.
8. Matsumiya LC, Lavoie C. An outbreak of *Pasteurella pneumotropica* in genetically modified mice: Treatment and elimination. *Contemp Top Lab Anim Sci*. 2003; 42(2):26-8.
9. Percy DH, Barthold SW. Mouse. In: *Pathology of Laboratory Rodents and Rabbits*, 4th ed. Ames, IA: Blackwell Publishing; 2016:66-67.
10. Picut CA, Swanson CL, et al. The metrial gland in the rat and its similarities to granular cell tumors. *Toxicol Pathol*. 2009; 37(4):474-480.
11. Sasaki H, Ishikawa H, Sato T, Sekiguchi S, Amao H, Kawamoto E, Matsumoto T, Shirama K. Molecular and virulence characteristics of an outer membrane-associated RTX exoprotein in *Pasteurella pneumotropica*. *BMC Microbiol*. 201; 11:55.
12. Towne JW, Wagner AM, Griffin KJ, Buntzman AS, Frelinger JA, Besselsen DG. Elimination of *Pasteurella pneumotropica* from a mouse barrier facility by using a modified enrofloxacin treatment regimen. *J Am Assoc Lab Anim Sci*. 2014; 53(5):517-22.
13. Ward GE, Moffatt R, Olfert E.J. Abortion in mice associated with

Pasteurella pneumotropica. *Clin Microbiol*. 1978; 8(2):177-80.

CASE III: EX54BF-1 or 2 (JPC 4035521).

Signalment: Eight-month-old female Balb/c mouse (*Mus musculus*).

History: The mouse is from another institute and was culled during routine surveillance.

Gross Pathology: There is an approximately 3cm diameter cystic subcutaneous mass in the ventral neck and cranial chest. The mass is composed of pale friable tissue and has a rich blood supply. When bisected, it contains a central cavity within which there is blood and viscous material. No other abnormalities were identified in the carcass.

Laboratory results: None

Histopathologic Description: (Participants will receive one of two slides: one sample is from the central region of the mass where it contains a large and partly collapsed central cavity. The second sample is smaller and more solid and was obtained from a lateral aspect of the mass).

There is a well-circumscribed multinodular and cystic subcutaneous mass composed of disorganized proliferation of plump spindle to polygonal cells arranged into interlacing fascicles, solid lobules and thick bands where the cells are often arranged in a palisade. The fibrovascular stroma is fine. The outline of the central cavity is irregular. It extends among lobules of neoplastic cells and contains a variable amount of necrotic debris and proteinaceous material. The neoplastic spindle cells have small to moderate amount of eosinophilic to amphophilic cytoplasm, indistinct cytoplasmic margins and oval finely granular nuclei with multiple small nucleoli. There is mild anisocytosis and anisokaryosis. In some areas, the cells are polygonal and have more abundant eosinophilic and often granular cytoplasm (some of these cells appear degenerate). The mitotic rate is approximately 0-2/HPF. The tumor compresses the surrounding tissue including the sublingual salivary gland and bundles of skeletal muscle. Mostly in the connective tissue around the tumor, there is moderate multifocal mononuclear infiltration and accumulation of some pigment-laden macrophages (hemosiderin, presumptive). In the outer region of the mass, there is multifocal fibrosis, which in some areas merges with a "compression capsule". At the periphery of the mass there is multifocal prolapse of neoplastic lobules into dilated veins (so-called "pseudoinvasion").

Contributor's Morphologic Diagnosis: Myoepithelioma

Ventral neck, Balb/c mouse: A 3cm cystic is present in the subcutis of the ventral neck which extends into the cranial aspect of the chest. Numerous cysts are visualized with bisected (bottom right). (Photo courtesy of: The Weizmann Institute of Science, Department of Veterinary Resources, http://www.weizmann.ac.il/vet/).

Contributor's Comment: Myoepithelial cells are ectoderm-derived modified epithelial cells found around acini and ducts of exocrine glands e.g. sweat glands, mammary glands, lacrimal glands and salivary glands.[2,5] They form a thin, basal layer between the basement membrane and the secretory cells of the luminal layer and are organized differently in ducts and alveoli.[2] In the former, they are arranged as a more or less continuous monolayer, whereas in the latter they are stellate shaped and their long branched cytoplasmic processes cradle the secretory unit like a loose basket.[2] Other than their involvement in mixed mammary tumors in dogs, primary tumors of myoepithelial cells are rare in domestic and laboratory animals.

In laboratory mice, myoepitheliomas are not uncommon but are usually limited to specific strains. The latest reference we found describing a relatively large group of these tumors in mice is Sundberg JP et al. *Vet Path* 28:313, 1991 which discusses myoepitheliomas diagnosed through routine surveillance of The Jackson Laboratory's production and research colonies. This is a study of 142 tumors in mice the majority of which were less than one-year-old. The following data is from this reference.

Myoepitheliomas occur spontaneously in strains A, Balb/c and their F1 hybrids. Most tumors were of salivary gland origin and the most common location was the ventral neck

(74%), as in the submitted case. Other locations included head (periorbital), perineum and ventral abdomen with origin from the salivary, Harderian, clitoral, preputial and mammary glands. The gender predisposition differed between the two strains. Balb/c females were predominantly affected whilst in A/J strain the reverse was true. In the Jackson study, the mean age at which tumors were detected was 234 days but other studies indicate that tumors arise predominantly in mice which are more than one-year-old. In the Jackson colony the frequency of malignancy, as determined by pulmonary metastases or invasion of underlying bone, was low (6%). A metastatic rate of >10% is reported in other studies of older mice, suggesting that the frequency of metastasis increases with age. Myoepitheliomas have been transplanted, but their etiology remains unknown. Virus particles were not identified in ultra-structural examination and molecular studies did not produce evidence implicating viral infection.[5]

The macroscopic and histologic appearance of myoepitheliomas appears to be fairly consistent and similar to the submitted case. [5] Grossly, the tumors were fluctuant, ranged in size from 0.5 - >4 cm in diameter and the single large central cavity contained opaque, odorless, pink to brown watery fluid. According to The International Classification of Rodent Tumors[1], the tumors are composed of pleomorphic cells that can resemble epithelial or mesenchymal cells. Adjacent to vessels, tumor cells tend to align themselves in an epithelial fashion. Multiple necrotic areas are present and mucoid material accumulates in pseudocysts as result of degeneration. The tumors can be invasive into surrounding tissue, and large tumors can metastasize to the lung.[2]

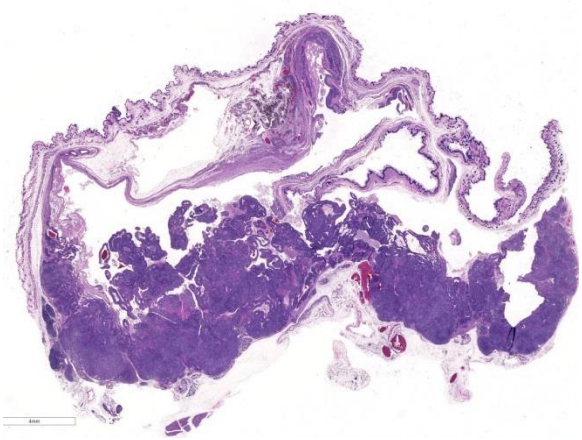

Ventral neck, Balb/c mouse: At subgross magnification, a densely cellular, cystic neoplasm is present within the subcutis. (HE 5X)

Immunohistochemical analysis showed that normal acinar and ductal myoepithelial cells and neoplastic cells were positive when stained with antibodies against cytokeratin, K5 and K14. Alpha-smooth muscle-1 antibody stained normal acinar myoepithelial cells but neither normal ductular myoepithelial cells nor neoplastic cells. This supports the notion that the tumors originate from ductular myo-epithelial cells.[5] Normal myoepithelial cells and neoplastic cells were negative for antisarcomeric actin, panmyosin, desmin, and S-100.[5]

JPC Diagnosis: Salivary gland: Myoepithelioma, Balb/c mouse, *Mus musculus*.

Conference Comment: Myoeptheliomas, also known as pleomorphic adenomas or benign mixed salivary gland tumors, are a relatively uncommon, spontaneously occurring salivary gland neoplasm in A strains and Balb/c mice, with a predilection for females.[4] Although typically considered to be benign, these neoplasms can grow tremendously and contain large cystic chambers containing necrotic cellular debris admixed with a mucinous secretory product. In humans, about 5% of myoepitheliomas undergo malignant transformation, but the

rate of malignancy in animal species is unknown. In mice, larger tumors can be aggressive with marked local invasion and metastasis to the lung.[3,4,5]

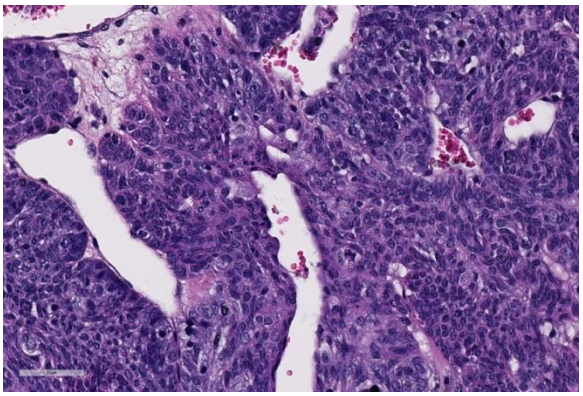

Ventral neck, Balb/c mouse: Neoplastic cells are spindled, and arrayed in small streams and bundles. Cells have a high N:C ratio. (HE 5X)

Myoepitheliomas can have a somewhat variable histomorphology but are typically composed of pleomorphic spindle cells that have features of both mesenchymal and epithelial cells.[4,5] As their name suggests, myoepithelial cells are contractile with both a smooth muscle and epithelial component, and myoepitheliomas are thought to be derived from the myoepithelial or ductal reserve cells of the salivary gland.[3,4,5] Normally, myoepithelial cells are located between the lumen and basal lamina of secretory structures, such as salivary glands, sweat glands, lacrimal glands, and mammary glands. The epithelial component of this neoplasm can form ducts or form nests of keratin-filled horn cysts, although that is not a striking feature in this case.[3,4,5] Myoepitheliomas have been reported infrequently in mammary glands in dogs, nonhuman primates, and humans. In mice, myoepitheliomas have been associated with salivary, mammary, preputial, and Harderian glands.[4] Conference participants agreed that the tumor is arising from the salivary gland based on the glandular or ductular profiles occasionally found in the neoplasm interpreted as preexisting salivary structures entrapped by neoplastic cells.

As noted by the contributor, there is significant slide variation in this case. This variability is due to the use of tissue from different parts of the neoplasm.

Contributing Institution:
The Weizmann Institute of Science
Department of Veterinary Resources
http://www.weizmann.ac.il/vet/

References:

1. Mohrs U, ed: *International Classification of Rodent Tumors: The Mouse*. Springer: Berlin; 2001:29.
2. Moumen M, Criche A, Cagnet S, Petit V Raymond K, Faraldo M, Dugnier MA, Glukohva MA. The mammary myoepithelial cell. *Int J Dev Biol*. 2011; 55:763-771.
3. Munday JS, Lohr CV, Kiupel M. Tumors of the alimentary tract. In: Meuten DJ, ed. *Tumors in Domestic Animals*. 5th ed. Ames, IA: Wiley Blackwell; 2017:853-855.
4. Percy DH, Barthold SW. Mouse. In: *Pathology of Laboratory Rodents and Rabbits*. 4th ed. Ames, IA: Blackwell Publishing; 2016:114-115.
5. Sundberg JP, Hanson CA, Roop DR, Brown KS, Bedigian HG. Myoepitheliomas in Inbred Laboratory Mice. *Vet Pathol*. 1991; 28:313-322.

CASE IV: AFIP 2013 (JPC 4039981).

Signalment: 19-year-old male rhesus macaque (*Macaca mulatta*).

History: This animal was part of a colony housed at the Texas Biomedical Research

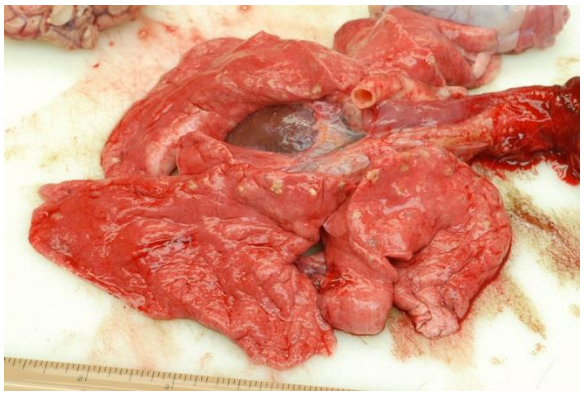

Lung, rhesus macaque. Numerous 2-5mm diameter tan nodules are present within all lung lobes. (Photo courtesy of: Covance Laboratories, Inc, Madison, Wisconsin, USA.
http://www.covance.com/products/nonclinical/toxicology/risk-assessment/index.php).

Institute. Clinical signs included chronic age-related arthritis in both knees and a general decline in condition associated with cachexia, diarrhea, and dehydration. The animal was euthanized due to poor condition.

Gross Pathology: External: The animal was dehydrated with low body fat but adequate muscle. Several teeth were missing. Both knees had reduced range of motion and periarticular thickening.

Internal: The liver was enlarged with pale tan edges on several lobes. The colon was distended with fluid feces. There was multifocal, 2-5 mm diameter, slightly raised tan nodules in all lung lobes.

Laboratory results: Simian retrovirus and herpesvirus serology were negative.

Histopathologic Description: Lung: Multifocally, bronchial and bronchiolar walls are irregularly thickened by large numbers of lymphocytes, plasma cells, macrophages, and eosinophils, with fewer neutrophils and multinucleated giant cells. Airway lumens are often enlarged and contain macrophages, granulocytes, and cross and tangential sections of arthropod parasites. Arthropods are approximately 300-500 um in width and characterized by a thin chitinized cuticle, jointed appendages, striated musculature, a body cavity, digestive tract, and reproductive organs. Many macrophages contain abundant intracytoplasmic golden-brown to black, finely granular, birefringent pigment (mite excrement). The inflammatory cell aggregates multifocally disrupt and/or obscure the bronchial and bronchiolar walls, form lymphoid follicles, variably compress or extend into adjacent alveolar tissue, and elevate the pleura (raised nodules noted grossly). Affected bronchi and bronchioles exhibit moderate smooth muscle hypertrophy and occasional peribronchiolar fibrosis. In less affected lung, terminal airways and alveoli are multifocally dilated with occasional loss of alveolar septa.

Lung, rhesus macaque. Numerous 2-5mm diameter tan nodules are present within all lung lobes. (Photo courtesy of: Covance Laboratories, Inc, Madison, Wisconsin, USA.
http://www.covance.com/products/nonclinical/toxicology/risk-assessment/index.php).

Contributor's Morphologic Diagnosis: Lung: Bronchitis/bronchiolitis, chronic and eosinophilic, multifocal, moderate, with bronchiolectasis, smooth muscle hypertrophy, and mites and mite pigment, etiology consistent with *Pneumonyssus sp*.

Other diagnoses in this animal included hepatic amyloidosis and chronic lympho-plasmacytic colitis.

Contributor's Comment: Although *Pneumonyssus simicola*, the lung mite of rhesus macaques, has become a less common parasite in most managed primate colonies; the incidence of pulmonary acariasis remains very high in feral and wild caught rhesus monkeys. Despite extensive microscopic findings in many affected animals, infection is typically subclinical. Sneezing, coughing, and dyspnea have been reported.[8] Antemortem diagnosis can be difficult. Radiographs are generally not helpful; however, tracheobronchiolar lavage has been a successful diagnostic tool, usually by identifying larva that migrates to the larynx. False negatives are possible.[1,4,5]

As demonstrated in the accompanying photographs, gross findings appear as multifocal and coalescing, discrete, irregularly round to ovoid, slightly raised, light brown foci several millimeters in size. In contrast to *M. tuberculosis*, the lesions of *Pneumonyssus simicola* are typically soft and cystic, or air-filled bullae.[1] Thin fibrous

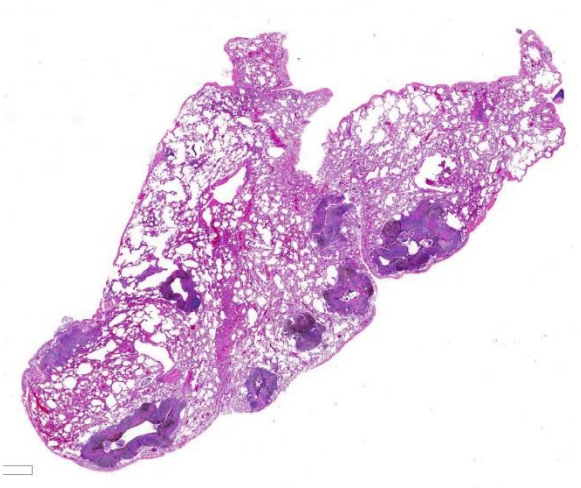

Lung, rhesus macaque. Bronchioles are ectatic and their walls are expanded by a dense cellular infiltrate. (HE, 5X)

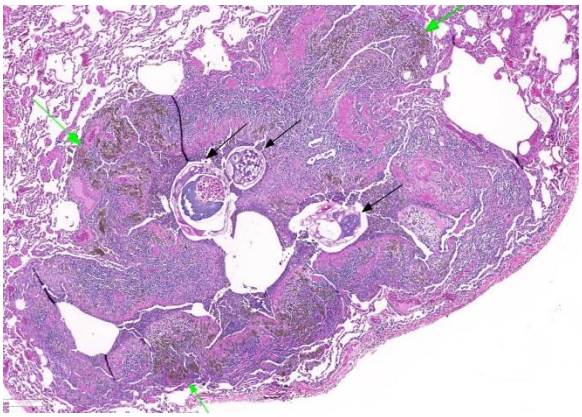

Lung, rhesus macaque. Walls of ectatic bronchioles are markedly expanded by lymphocytes and plasma cells, and aggregates of macrophages containing a dark brown pigment (green arrows). The lumen contains cross sections of numerous arthropod parasites (black arrows), surrounded by cellular debris. (HE, 57X)

adhesions within the pleural cavity are commonly observed.[9]

Microscopic lesions consist of multifocal chronic bronchiolitis and bronchiolectasis with hyperplasia of bronchiolar smooth muscle and prominent peribronchiolar lymphoid aggregates admixed with eosinophils and pigment-laden macrophages. Adult mites, most of which are females, are normally evident in sections of affected lung. Mites are identifiable by typical arthropod characteristics; a chitinized outer cuticle, body cavity, striated musculature, jointed appendages, and sometimes other structures including brain, gastrointestinal and reproductive tract, eggs and occasionally larvae. The presence of birefringent brown to black pigment in macrophages at the periphery of affected bronchioles is a hallmark of infection and considered diagnostic even in the absence of identifiable mites.[8]

JPC Diagnosis: Lung: Bronchiolitis and bronchitis, pyogranulomatous and eosino-philic, chronic, multifocal, moderate, with bronchiectasis and bronchiolar intraluminal

arthropods with mite pigment, rhesus macaque, *Macaca mulatta*.

Conference Comment: The contributor provides an outstanding example of pulmonary acariasis in a nonhuman primate, with numerous cross sections of well-preserved adults and eggs scattered throughout the larger conducting airways in this section of lung. *Pneumonyssus simicola* mites are ubiquitous in wild and wild-caught Old World primates with an incidence of nearly 100%.[2,3,9] As a result, mites and their associated lesions are considered a background incidental finding in these animals.[2,9] Previously reported pulmonary histologic lesions are generally similar to this case with eosinophilic to granulomatous bronchitis/bronchiolitis with variable amounts of brown to black mite pigment within bronchi and bronchioles and moderate to marked inflammation expanding the peribronchiolar interstitium.[2,9]

Other than the abundant mite pigment, conference participants agreed that the most striking histologic lesion is the profound bronchiectasis. Bronchiectasis is the permanent marked dilation of bronchi and is a consequence of chronic bronchial obstruction by the parasite.

As described by the contributor, adult mites have the typical arthropod characteristics of 300-500 um width, chitinous exoskeleton, mouth parts, jointed appendages, striated musculature, a body cavity, digestive tract, reproductive structures, yolk material in yolk glands, and developing eggs.[3] The highly characteristic birefringent golden brown to black crystalline mite pigment, thought to be a metabolite of digestion and excretion by the female mite, can be present in sections that lack mites and are diagnostic for the parasite.[2,3,9] This pigment does not contain melanin or carbon, but rather is composed predominantly of iron. This the

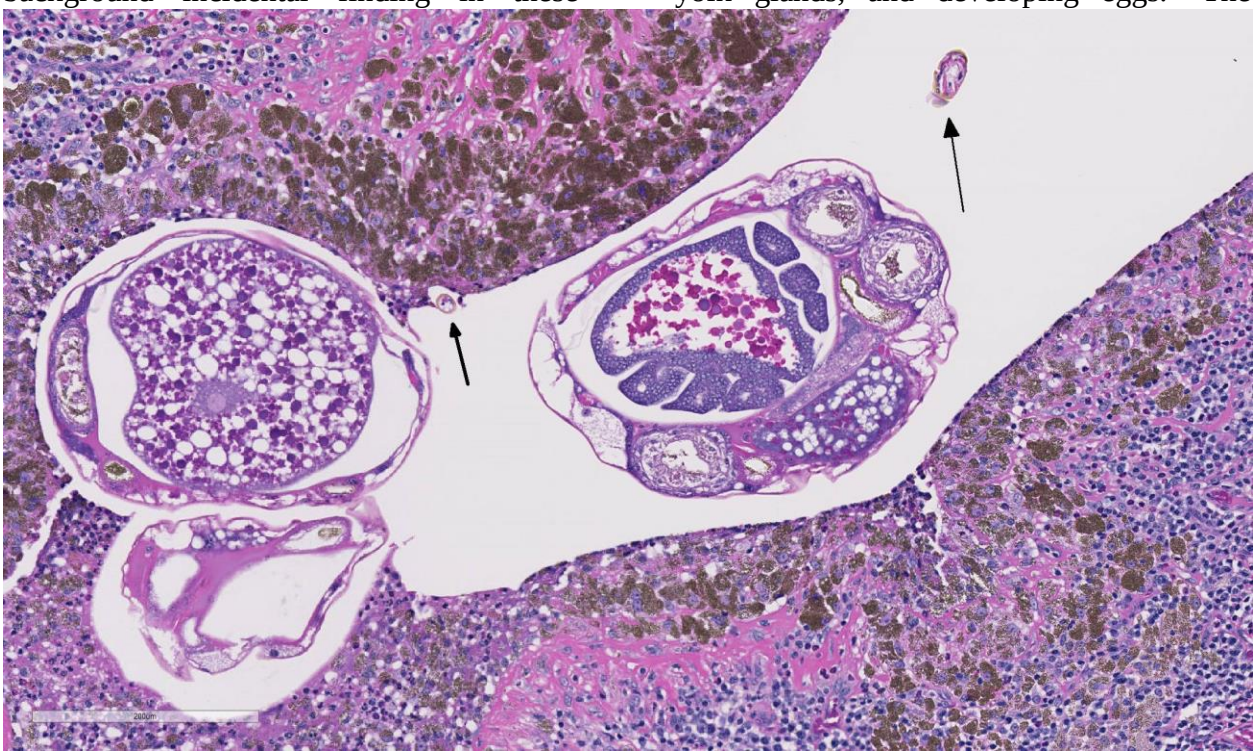

Lung, rhesus macaque. Higher magnification of lung mites (Pneumonyssus simicola) which demonstrates jointed appendages surrounded by a chitinous exoskeleton (black arrows), and digestive and reproductive tracts of the parasites. (HE, 125X)

result of the mite feeding on host erythrocytes with digestion and excretion of blood protein, hemoglobin.[9] Additionally, mite pigment is likely the cause of the majority of the inflammatory response within the lungs.[2] Widespread use of the anthelmintic medication, ivermectin, during quarantine of new animals and as a part of routine colony management has markedly reduced the incidence in laboratory nonhuman primates.[2,9]

Pulmonary acariasis and nasopharyngeal mites occur in many other animal species. Some of the most important nasal and pneumotropic arthropod parasites of veterinary importance include *Pneumo-nyssoides* sp. in the lungs of New-world primates; *Rhinophaga* sp. in the nasal cavity of Old-world primates; *Pneumo-nyssoides caninum*, the nasal mite in dogs; *Linguatula serrata* in the nasal cavity of dogs and cats; *Oestrus ovis*, the nasal botfly in sheep and goats; *Entonyssus* sp. and *Entophionyssus* sp. in the trachea and lung of snakes; *Cephenemyia* sp. in the nasal cavity of wild cervids; *Cytodites nudus* in the air sacs of poultry; and *Halarachne halichoeri* in the nasal passages of wild sea lions.[6]

Contributing Institution:
Covance Laboratories, Inc
Madison, Wisconsin, USA.
http://www.covance.com

References:

1. Andrade MCR, Marchevsky RS. Histopathologic findings of pulmonary acariasis in a rhesus monkeys breeding unit. *Revista Brasileira de Parasitologia Veterinária*. 2007; 16(4):229-234.
2. Cogswell F. Parasites of non-human primates. In: Baker DG, ed. *Flynn's Parasites of Laboratory Animals*. 2nd ed. Ames, Iowa: Blackwell Publishing; 2007:716-717.
3. Gardiner CH, Poyton SL. *An Atlas of Metazoan Parasites in Animal Tissues*. Washington, DC: Armed Forces Institute of Pathology; 1999:56-58.
4. Keeling M, Wolf R. Respiratory diseases. In: Bourne G, ed. *The Rhesus Monkey, Volume II: Management, Reproduction, and Pathology*. New York, NY: Academic Press; 1975:70-71.
5. Lowenstine LJ, Osborn KG. Respiratory system diseases of nonhuman primates. In: Abee C, Mansfield K, Tardif S, Morris T, eds. *Nonhuman Primates in Biomedical Research: Diseases*. London, UK: Academic Press; 2012:467-468.
6. *Pneumonyssus simicola*. Joint Pathology Center Systemic Pathology (updated Oct. 2014). Retrieved from: https://www.askjpc.org/vspo/show_page.php?id=595.
7. Purcell JE, Philipp MT. Parasitic diseases of nonhuman primates: In Wolfe-Coote S, ed. *The Laboratory Primate*. San Diego, CA: Elsevier; 2005:589-590.
8. Stookey J, Moe J. The respiratory system. In: Benirschke K, Garner F, Jones T, eds. *Pathology of Laboratory Animals*, Vol. 1. New York, NY: Springer-Verlag; 1978:106-107.
9. Strait K, Else JG, Eberhard ML. Parasitic diseases of nonhuman primates. In: Abee CR, Mansfield K, Tardiff S, Morris T, eds. *Nonhuman Primates in Biomedical Research: Diseases*. 2nd ed. Vol. 2. San Diego, CA: Academic Press;